BMW Airhead Oil Filter Canister Displacement: Service Practice, Load Paths, and the $2,000 O-Ring Myth

Custom Konrad

January 10, 2026

Abstract

At the conclusion of an extensive rebuild of a 1983 BMW R80ST—including electrical, ignition, charging, and mechanical upgrades—the engine started immediately and ran as expected. Shortly thereafter, oil leakage was observed at the oil filter cover, implicating the BMW Airhead's well-known and notoriously sensitive oil filter sealing system, colloquially referred to as the "$2,000 O-ring."

Although the symptoms initially resembled common seal preload or elastomer creep failure modes, investigation revealed a more prosaic root cause. The fastener located beneath the oil filter canister mouth is *always* short by design on this engine family, independent of oil pan configuration. In this case, an overlong fastener was incorrectly installed, allowing unintended contact with the canister and introducing a radial jacking load at the canister mouth.

While the immediate issue was resolved by mechanically re-centering the canister—a field-normal repair—residual plastic deformation at the canister mouth, combined with the precision nature of the sealing interface and the availability of a mechanically superior later canister design, motivated a deliberate decision to proceed beyond restored operability.

This case study traces the diagnostic path from symptom to root cause, examines the geometry and tolerance sensitivity of the BMW Airhead oil filter canister system, and analyzes canister retention, service tooling, and depth control. Particular attention is given to misconceptions regarding press-fit behavior, differences between early and later replacement canister designs, and a BMW parts fiche mislabeling that can complicate service. The incident serves as both a technical analysis and a cautionary example, underscoring the importance of fastener-length control, load-path awareness, and disciplined decision-making when modifying legacy mechanical systems.

1 Primary References and How to Reproduce Key Findings

Three complementary sources anchor this work, spanning parts identification, formal technical analysis, and practical service procedure. These references are cited throughout where applicable.

- **MaxBMW parts fiche (navigation path).** Navigate to MaxBMW Fiche: DiagramsMain.aspx, select `11 -- Engine`, and open `Diagram #11_1688`. In this diagram, the oil filter canister is identified as item `13`. While the associated part number (`11 11 1 338 203`) is correct, the description is incorrectly listed as "`STEERING COLUMN TUBE`." This mislabeling can cause confusion when relying solely on fiche-based identification, but was readily resolved through consultation with an experienced supplier such as **Max BMW Motorcycles**.
- **Largiader technical note on canisters and shimming.** See `largiader.com/tech/filters/canister.html`. This reference provides a detailed discussion of early versus later canister designs, O-ring and shim stack geometry, and depth-control practices, including quantitative guidance and tabulated recommendations.
- **Brooks & Brandon, *Airhead Garage* (procedural reference).** See the YouTube video "BMW Airhead Oil Filter $2000 O-Ring Explained". This source presents an experience-driven visual walk-through of oil filter and canister service, illustrating correct assembly order, common failure modes, and the practical consequences of tolerance mismanagement.

2 Background and Modification Context

The BMW Airhead oil filter system relies on a thin-wall steel canister installed into a deep cylindrical bore in the aluminum crankcase. Proper sealing is achieved by axial compression of a large elastomer O-ring at the canister mouth, optionally supplemented by one or more shims. The system is highly sensitive to canister depth (i.e., the distance from the crankcase face to the canister mouth), with acceptable variation on the order of tenths of a millimeter (see Largiader). Any axial displacement of the canister directly affects O-ring preload and seal integrity.

One of the oil pan fasteners is located immediately beneath the oil filter canister mouth. By design, this fastener is intentionally short in *all* configurations—whether a stock oil pan is installed or a distance ring and skid plate assembly is fitted—to prevent intrusion into the filter cavity and contact with the canister.

3 Observed Symptoms

Following completion of the rebuild—including installation of a Silent Hektik ignition (Z2070 Microlino), three-phase regulator/rectifier (R1335eco), and alternator (V1335 LiMa)—the engine was started after a prolonged period of non-operation. The engine started immediately and ran smoothly, with nominal ignition timing, charging behavior, and idle quality. However, oil leakage developed at the oil filter cover shortly after startup as crankcase pressure increased.

Given the extended downtime and the well-known sensitivity of the Airhead oil filter sealing system, the initial diagnosis focused on loss of O-ring preload or elastomer creep, consistent with the familiar "$2,000 O-ring" failure narrative.

4 Root Cause Discovery

The O-ring visible in Fig. 1 appears nominal and is included primarily for reference. Its mechanical role is indirect but decisive: once local support at the canister mouth was compromised, the O-ring—effectively incompressible in volume—continued to transmit its axial preload into the seal stack. With the load path constrained by the surrounding geometry, this preload was redistributed into the unsupported portion of the shim, producing smooth local plastic bending without requiring global overload or gross misalignment. In this condition, the O-ring transitions from a compliant sealing element to an effective load-transmitting medium.

To place the observed deformation behavior on a physically meaningful footing, the following analysis is presented as a *force-scale sanity check*, not as a seal design calculation.

Order-of-magnitude estimate of localized O-ring load transmission. Using standard O-ring compression-load data for a 70A elastomer, a circular O-ring with 4 mm cross-section subjected to 10–25% squeeze typically develops a compressive line load on the order of $f \approx 20$–90 lbf/in of circumference at room temperature.[1] For the present geometry, with center diameter $D_c = 50$ mm and circumference $L = \pi D_c = 157$ mm $= 6.19$ in, this corresponds to a total stored compressive force of

$$F_{\text{total}} = fL \approx 0.55\text{–}2.5 \text{ kN}.$$

If uniform backing is lost and the O-ring load is instead transmitted through only a fraction α of the circumference, the effective local line load increases approximately as $f_{\text{local}} \approx f/\alpha$. For a plausible localization $\alpha = 0.10$–0.25 and an estimated contact patch width $w \sim 1$ mm, the implied local contact pressure scales as

$$p_{\text{local}} \approx \frac{f_{\text{local}}}{w},$$

yielding pressures in the tens of megapascals even before accounting for further geometric concentration. Although operation at 100°C reduces the effective modulus of the elastomer, the qualitative conclusion remains unchanged: loss of backing strongly amplifies local stress transmission.

The susceptibility of the stainless shims to plastic deformation can be assessed by modeling a $t = 0.3$ mm shim as a thin strip spanning a locally unsupported region of width ℓ. For a simply supported strip under uniform pressure p, the maximum bending stress is

$$\sigma_{\max} \approx \frac{3p\ell^2}{4t^2},$$

from which the pressure required to reach yield may be estimated as

$$p_y \approx \frac{4\sigma_y t^2}{3\ell^2}.$$

Taking a representative stainless yield strength of $\sigma_y \approx 200$ MPa gives $p_y \approx 24$ MPa for $\ell = 1$ mm and $p_y \approx 6$ MPa for $\ell = 2$ mm. These values fall well within the range of localized pressures implied above, demonstrating that once uniform backing is compromised, even modest nominal O-ring squeeze can generate sufficient localized stress to plastically dish or dent thin metallic shims. In this regime, the O-ring no longer acts solely as a compliant sealing element, but functions as an effective load-transmitting medium.

[1] Values are consistent with published compression-force guidance for 70A elastomers; elevated temperature effects are addressed below.

Comparison to oil-pressure-induced separation force. The force transmission capacity implied by the O-ring preload can be placed in context by comparing it to the hydraulic force generated by normal engine oil pressure. For a static axial face seal, pressure containment requires that the local O-ring contact pressure exceed the fluid pressure along the sealing line; however, a gross force comparison provides a useful upper bound on the separation tendency.

A conservative estimate of the pressurized area may be obtained by taking the area enclosed by the O-ring inner diameter. For a circular O-ring with center diameter $D_c = 50\,\mathrm{mm}$ and cross-section diameter $d = 4\,\mathrm{mm}$, the inner diameter is approximately

$$D_{\mathrm{ID}} \approx D_c - d = 46\,\mathrm{mm}.$$

The corresponding pressurized area is

$$A_p \approx \frac{\pi}{4} D_{\mathrm{ID}}^2 = \frac{\pi}{4}(46\,\mathrm{mm})^2 \approx 1.66 \times 10^{-3}\,\mathrm{m}^2.$$

For a representative hot-oil operating pressure in the range $\Delta p = 4 -- 6\,\mathrm{bar}$, the resulting hydraulic separation force is

$$F_p = \Delta p\, A_p \approx (0.4 -- 0.6\,) \times 10^6\ \mathrm{Pa} \times 1.66 \times 10^{-3}\,\mathrm{m}^2 \approx 660 -- 1000\,\mathrm{N}.$$

This force scale is comparable to, but generally lower than, the total stored compressive preload in the O-ring estimated above ($F_{\mathrm{total}} \approx 0.55 -- 2.5\,\mathrm{kN}$ for 10–25% squeeze). More importantly, sealing is governed by *local contact pressure* rather than by net force balance. Typical O-ring contact stresses under nominal squeeze lie in the multi-megapascal range, whereas engine oil pressure remains well below 1 MPa. Consequently, under correct geometric support and load termination, the O-ring easily contains the applied oil pressure with substantial margin.

This comparison reinforces the central conclusion of this analysis: the observed failure does not arise from insufficient pressure capacity of the O-ring, but from a change in load path and backing conditions that redistributes O-ring preload into unsupported regions. Once axial support is locally compromised, even normal operating pressures and modest nominal squeeze are sufficient to drive extrusion and secondary shim deformation.

Further inspection identified radial interference between the oil filter canister and an overlong oil pan fastener located beneath the canister mouth. During installation, slight resistance was felt while tightening this fastener. This resistance was initially interpreted as normal thread engagement but is more consistently explained as the onset of lateral contact between the fastener tip and the thin-wall steel canister, introducing an unintended radial jacking load.

The mechanical response of the canister to this interference is documented in Fig. 2(a–c). After removal of the fastener, partial elastic spring-back was observed, but the canister did not fully re-center on its own. Deliberate mechanical re-centering at the mouth was required to restore alignment, indicating that the dominant response was rigid-body motion rather than purely elastic deformation.

Because the canister passes through the proximal crankcase wall with radial clearance and is constrained only at a distal press-fit region, radial interference at the mouth produces local lateral displacement and slight angular rotation of the canister, effectively pivoting about the distal bore. This motion does not primarily unload the O-ring; instead, it compromises the axial backing normally provided to the thin metal shim at the canister mouth.

With axial support locally compromised, the O-ring continues to transmit its preload into the seal stack, as quantified above. Because the shim is no longer uniformly backed, this force is applied over a reduced and asymmetric area, causing the unsupported portion of the shim to plastically deform and translate axially. The resulting axial motion drives the elastomer laterally into the annular gap between the canister and the crankcase face, producing the observed external oil leak.

The leak therefore arises not from global loss of O-ring preload, but from a change in load path and local support conditions that allow a radially initiated disturbance to manifest as axial seal extrusion.

Distinguishing rigid-body motion from localized yielding is difficult *in situ*; however, both mechanisms are consistent with the observed seal extrusion shown in Fig. 1. The demonstrated ability to re-center the canister (Fig. 2) strongly supports a lightly retained, non-heroic press-fit rather than a rigidly fixed component.

5 Why This Failure Mode Is Subtle

This failure mode is particularly insidious because it combines multiple well-known Airhead narratives:

- Symptoms closely resemble common seal preload or elastomer creep issues.
- The engine continues to run normally.

- The initiating cause lies outside the expected seal load path, even though it is physically adjacent to the leak location.

In this case, the presence of a visibly damaged and displaced O-ring reinforced an incorrect initial diagnosis focused on elastomer behavior. Only after recognizing the canister displacement and explicitly tracing axial load paths through the surrounding structure was the true cause identified.

Ironically, the resulting external oil leak served as a protective failure mode. Continued operation with a compromised seal may have prevented more serious internal bypass conditions by providing an early, visible indication of system distress.

Intentional Deviation from Field-Normal Repair

The immediate mechanical issue was resolved by re-centering the canister, a field-normal repair consistent with long-standing independent service practice. Nominal alignment was restored, and the system could have been reassembled and returned to service, as illustrated in Fig. 2. In many cases, this outcome would represent a reasonable and sufficient repair.

However, inspection revealed residual plastic deformation at the canister mouth. Although modest in magnitude, this deformation implied a permanent loss of roundness: once yielded, the mouth would no longer represent a pristine cylindrical reference. Any subsequent measurement of canister depth, shim stack height, or O-ring compression would therefore be referenced to a geometry that had already been compromised.

Because the canister mouth defines a precision sealing interface—one that must be evaluated by measurement rather than visual inspection—this residual deformation introduced an unacceptable degree of uncertainty. Even small geometric deviations could bias depth measurements, obscure loss of margin, or complicate future service decisions. For this reason, continued use of the deformed canister was judged to carry avoidable risk, despite the absence of immediate functional symptoms.

This assessment was reinforced by photographic documentation presented by Largiader, which illustrates the mechanically superior geometry of the later-style oil filter canister. The later design features a broader, flared, and axially flattened mouth that distributes contact pressure more uniformly and provides more stable backing for the O-ring and shim stack. In contrast, the earlier straight-cut geometry concentrates load at a relatively sharp edge, offering little tolerance once yielding initiates. In configurations where shims are not required, this sharp edge is inherently less stable: it promotes localized indentation, can abrade the

O-ring under compression, and provides no geometric mechanism for re-centering or load redistribution.

Practical considerations also informed the decision. With the motorcycle already out of service during the winter season, the additional analysis and corrective effort imposed minimal opportunity cost, allowing a more conservative, geometry-first approach without sacrificing riding time.

What initially presented as an assembly error was therefore reframed as an opportunity to replace a compromised component with a demonstrably better design. The analysis that follows reflects a deliberate choice to proceed beyond restored operability in order to establish a clean geometric baseline, quantify retention behavior, and replace service folklore with mechanically grounded understanding.

6 Canister Retention and Force Scale

The BMW Airhead oil filter canister is commonly described as a press-fit sleeve. Practical inspection and handling in this case reveal a more nuanced reality: the canister is positively retained, but not in a manner consistent with a heavy, blind-hole interference press that would be effectively immovable once seated.

Rather than behaving as a rigidly locked insert, the canister exhibits limited compliance consistent with a deliberate light-retention strategy. This approach balances axial stability, serviceability, and protection of the aluminum crankcase bore in a deep, slender geometry, where overly aggressive interference would invite bore damage, canister distortion, or impractical service forces.

6.1 Observation Versus Assumption

Several direct observations constrain the plausible retention model:

- After displacement, the canister could be rocked and re-centered.
- Re-centering required controlled leverage applied at the mouth (using a tire iron). The applied *moment* was perceptible due to the available torque arm, but the operation did not require impulsive loading, hammering, or high insertion force.
- No evidence of bore galling, fretting, or elevated contact stress was observed on either the crankcase bore or the canister surface.

These observations are incompatible with a long, high-interference press-fit acting along the full engagement length. Instead, they point to a retention scheme dominated by a relatively short interference region or localized contact band that provides adequate axial stability while remaining serviceable and mechanically forgiving.

6.2 Constraint Geometry and the Effective Retention Model

A critical geometric point—often obscured by simplified descriptions—is that the canister is not guided by a long, close-fitting bore extending from the crankcase face inward.

Proximally, the canister passes through the entry crankcase wall with visible radial clearance. Meaningful constraint occurs only distally, where the canister engages a press-fit region deeper within the case. This topology implies that lateral interference at the mouth can induce local lateral displacement and slight angular rotation, with the sleeve responding as a constrained element pivoting about a distal retention zone rather than translating within a continuous tube.

This distinction is central to the observed failure: a radially applied disturbance at the mouth can alter local support conditions and backing geometry without requiring large axial motion or global loss of retention.

6.3 Retention Force: Order-of-Magnitude Estimate

Precise quantification of sleeve retention force would require detailed knowledge of local interference, contact length, surface finish, and friction state. However, the observed ability to re-center the canister using controlled leverage—together with the absence of galling or surface damage—supports a *light-retention* interpretation.

For force-scale reasoning, it is reasonable to place the axial retention force in the sub-kilonewton range. In this work, an order-of-magnitude estimate of

$$F_{\text{ret}} \sim 200 -- 800\,\text{N}$$

is adopted as a physically plausible bound for a lightly retained steel sleeve in an aluminum bore with lubricated contact. The intent is not to assert a measured value, but to establish a force scale consistent with the observed handling behavior and the absence of heroic extraction or installation tooling.

6.4 O-ring Behavior and Load Termination

The O-ring used in the BMW Airhead oil filter system is effectively incompressible in volume: it deforms readily, but does not compress in the volumetric sense. Consequently, the condition in which the O-ring fully occupies its available gland volume represents a *limiting case*, not a design objective.

Optimal sealing occurs short of volumetric lock-up. As gland fill approaches unity, local contact pressures rise sharply and sensitivity to geometric error increases. Beyond this threshold, incremental displacement or load can no longer be accommodated by benign shape change and is instead redirected into adjacent components, increasing the risk of shim deformation, extrusion, or elastomer damage.

In the nominal configuration, the sealing load path is deliberately terminated by geometry: once the O-ring is deformed into its intended operating range and the cover contacts a hard stop (either the crankcase face or a shim-defined interface), further bolt torque increases fastener tension rather than seal or canister load. The failure mechanism described in Section 4 arises precisely because this termination condition was locally defeated.

6.5 Shim Selection as a Goldilocks Problem

The objective of the final configuration is not merely restored operability, but a robust, measurable, and repeatable sealing geometry. The adopted two-shim solution increases stack height by 0.6 mm relative to a zero-shim baseline, placing the O-ring within its intended deformation band as discussed in Section 9.

The BMW Airhead oil filter sealing system does not reward monotonic conservatism. It is a true Goldilocks problem: insufficient stack height reduces O-ring squeeze and sealing margin, while excessive stack height drives the system toward volumetric lock-up, elevated local stresses, and loss of geometric load termination. Adding a shim does not inherently increase safety; it moves the operating point along a narrow corridor bounded on one side by leakage and on the other by overconstraint, shim distress, and elastomer damage.

Accordingly, the corrected installation prioritizes:

- restoration of a clean, round canister mouth,
- uniform and symmetric axial backing for the shim,
- and deliberate shim selection that achieves controlled O-ring deformation without approaching volumetric lock-up.

Depth measurement and geometric verification are therefore indispensable. The system cannot be tuned reliably by intuition alone; it demands quantitative placement within a small but stable operating window.

7 Canister Geometry: Old Versus New (Largiader + As-Received Observations)

Largiader documents two oil filter canister designs and discusses their implications for O-ring and shim stack behavior and depth control. These descriptions provide useful conceptual context; direct inspection and measurement in the present case further refine those distinctions.

Commonly cited design differences include:

- **Earlier design**: thicker nominal wall section (order 1.5 mm) with a comparatively simple, straight-cut mouth geometry.
- **Later design**: thinner nominal wall section (order 1.0 mm) with a formed mouth that increases axial stiffness and provides a broader sealing land for the O-ring and optional shims.

Contrary to some secondary descriptions, direct measurement of multiple canisters did not reveal a reliable or repeatable axial length difference between earlier and later parts. Measured values clustered around 137.7 mm, with observed differences (e.g. 137.87 mm versus 137.63 mm) falling within expected manufacturing tolerance and measurement uncertainty. There is therefore no evidence to support a designed length reduction or a systematic tendency for newer canisters to seat deeper as a function of axial length alone.

The mouth geometry of the later-style canister is best described as a multi-step forming process: the thin wall is flared outward, rolled inward, and then flattened axially. This sequence produces a substantially thicker and stiffer sealing land than a simple straight-cut edge, improving O-ring support, load distribution, and resistance to local deformation under axial preload.

An additional geometric consequence of the earlier straight-cut canister design is its narrower axial sealing land at the mouth. This geometry permits greater local radial displacement before contact is arrested and presents a larger effective elastomer migration footprint once deformation begins. In contrast, the later-style canister's wider, folded mouth limits radial excursion and concentrates contact over a smaller active area, while simultaneously providing substantially higher local stiffness. Because the enlarged mouth reduces the available radial clearance, any intrusion produces contact sooner and converts additional fastener rotation more directly into reaction force, causing abnormal installation torque to rise more steeply and be felt earlier by the operator.

From a service perspective, this increased stiffness has a secondary but relevant implication: intrusion by an overlong fastener into the later canister design would be expected to generate higher installation resistance at an earlier stage, increasing the likelihood that abnormal contact is detected by the operator. The earlier design, by contrast, is more compliant at the mouth and provides less geometric constraint against small radial disturbances, offering fewer early cues of backing loss. Once axial support is locally compromised, the narrower straight-cut mouth leaves a larger adjacent annular void, giving the O-ring greater opportunity to extrude laterally into the gap between the canister and the crankcase face.

This difference should not be interpreted as implying that interference is "silent" during assembly—in the present case, installation resistance was distinctly abnormal and should have been treated as a stop condition. The practical implication is instead a force-scale one: the folded mouth of the later-style canister is structurally far stiffer, and achieving comparable radial displacement at the mouth would be expected to require substantially larger jacking forces (and therefore much higher fastener torque), making meaningful mouth deformation increasingly difficult without extreme, self-evidently incorrect installation effort.

7.1 As-Received Replacement Canisters (This Case)

Two replacement canisters were obtained as BMW part `11 11 1 338 203`. Both were visually consistent with the intended oil filter canister design and with each other.

The identical distal geometry and outer diameter indicate that interference fit behavior is governed primarily by nominal diameter and surface finish rather than by local distal features. No conclusions can be drawn regarding compatibility with specific extraction tools based on distal geometry alone.

Field context. Independent BMW specialists have long noted variability in effective installed canister depth arising from crankcase machining tolerance, prior service history, and seating behavior rather than from intentional design changes in canister length. These observations reinforce the importance of direct depth measurement and controlled installation over reliance on nominal part descriptions.

8 Replacement Part Identification Anomaly (MaxBMW Fiche)

Replacement canisters are supplied under BMW part number `11 11 1 338 203`. In the MaxBMW fiche navigation described in Section 1, this part is correctly listed under item `13` of `Diagram #11_1688`, but is incorrectly described as *"STEERING COLUMN TUBE."*

Despite the incorrect description, the part number itself is correct and does correspond to the oil filter canister. While this mislabeling can cause momentary confusion when relying solely on fiche descriptions, it does not reflect an actual parts ambiguity once the number is traced correctly.

Independent fiche verification. The fiche discrepancy and final part identification were independently verified through consultation with **Max BMW Motorcycles**. Confirmation of the correct canister variant based on VIN and production date resolved the catalog inconsistency and enabled timely procurement despite the winter holiday period.

9 Canister Depth Control Strategy (Largiader-Aligned)

Given the sensitivity of the seal stack to axial placement, the most robust depth-control strategy is to reference the *installed depth of the original canister*, rather than relying on nominal drawing values or assumed axial stops. Because the original and replacement canisters share the same overall length and geometry, effective depth control is achieved by controlled installation relative to the original seating condition.

Any residual variation can then be accommodated at the canister mouth using standard external shims, which remain directly observable and adjustable during assembly. A critical constraint is the avoidance of a *proud* canister condition, which could introduce unintended axial contact or preload at the bore end and compromise seal behavior. Accordingly, depth control should be achieved through measurement, seating discipline, and external shimming alone.

Background observations. Independent service experience, including long-running shops such as **Duncan's Beemers**, has repeatedly highlighted oil filter canister depth as a non-trivial variable influenced by crankcase machining tolerance, service history, and seating behavior. This reinforces the need for explicit depth measurement and control rather than reliance on nominal dimensions or assumed axial stops.

9.1 Percent O-Ring Compression as a Secondary Check

In addition to groove-depth and stack-height methods, some practitioners evaluate the oil filter seal using a percent O-ring compression metric. This approach is commonly presented in instructional material from Brooks & Brandon's *Airhead Garage* and appears in various community references.

The compression percentage is computed as

$$\%\,\text{compression} = \frac{O + nS - C - D}{O} \times 100\%, \tag{1}$$

where:

- O is the O-ring cross-section thickness (nominally $\sim$4.0 mm for the white O-ring),
- n is the number of shims,
- S is the thickness of each shim (nominally 0.3 mm),
- C is the oil filter cover gasket thickness (typically $C = 0$ in modern practice, as the gasket is often omitted),
- D is the measured canister depth from the crankcase face.

A commonly recommended acceptance band is 10–25% compression, which corresponds to approximately 0.4 ——1.0 mm of O-ring squeeze when $O = 4.0$ mm. This range overlaps with, and is broadly consistent with, the groove-depth guidance documented by Largiader.

Percent O-ring compression is included here only as a secondary consistency check. By construction, it cannot detect loss of axial backing caused by radial canister displacement, since such displacement alters load paths without necessarily changing the nominal compression value. In the present case—precipitated by an unforced assembly error upstream of the sealing interface—numerically acceptable compression would have been computed even though the sealing geometry had already been compromised. This limitation does not diminish the utility of the method under normal conditions, but it underscores that compression checks assume intact canister geometry and are not diagnostic of upstream mechanical interference.

10 Removal and Installation Tooling: Practical Reality

Oil filter canister service requires controlled axial force applied through positive mechanical engagement while maintaining alignment in a deep, blind bore. Friction-only methods are unreliable and risk secondary deformation or bore damage.

Observed canister mobility indicates that the required axial forces are moderate in magnitude; however, successful extraction depends far more on *alignment control and tactile feedback* than on raw force capability.

10.1 Field-Expedient Extraction Method (As Executed)

In principle, a purpose-designed internal puller that positively engages a distal shoulder would be an attractive solution. In practice, the as-installed canister and all observed replacement canisters lacked robust distal cut-outs, shoulders, or undercuts suitable for conventional internal-jaw pullers. While a distal screw-based puller could be imagined, it would require an extremely shallow, sharp engagement lip and precise geometry; it is not clear that such a tool is feasible or that one exists. No commercially available or commonly cited example is known to the author.

Given these constraints, extraction in this case was performed using a controlled drive-out method enabled by a single radial hole in the canister wall.

Concept. A radial hole is drilled through the thin canister wall at an accessible location. A steel screw (or closely fitting pin) is inserted through the hole to act as a temporary drive feature. Axial extraction force is then applied by tapping on this feature *while simultaneously applying counter-torque and alignment control at the canister mouth*. These actions are not sequential; they occur continuously and in concert.

Important safety note. This method carries inherent risk and should not be treated as a generic procedure. Specific hazards include: (i) generation of metal chips near the oil system, (ii) risk of drilling into the aluminum crankcase if depth control is lost, and (iii) risk of cocking the canister and damaging the bore. Execution relies heavily on operator judgment, tactile sensitivity, and continuous control rather than prescriptive steps.

Procedure outline (conceptual, high level).

1. **Access and preparation.** Remove components as needed to obtain clear access to the canister and lower cavity. Clean the work area and establish chip-capture measures (grease, rags, shielding, suction, and post-operation flushing).

2. **Hole placement and drilling.** Select a location clearly within the thin-wall region of the canister (not through the rolled mouth). Drill only through the canister wall, using positive depth control. The intent is to create a controlled drive feature, not a structural modification.

3. **Simultaneous extraction and alignment control.** Insert a steel screw or pin through the hole. Apply light tapping force to the drive feature while *simultaneously* applying reactive counter-torque at the canister mouth using a lever (e.g., a tire iron). The operator can feel the upward axial reaction moment transmitted through the counter-torque tool. Tapping, alignment correction, and axial guidance occur continuously and together, not as discrete steps.

4. **Continuous tactile monitoring.** The canister's motion, resistance, and tendency to tilt are assessed continuously through feel. Any increase in side resistance or loss of smooth axial motion requires immediate corrective action. The objective is to maintain predominantly axial translation throughout the process.

5. **Completion and inspection.** Once released, remove the canister by hand. Carefully remove all chip containment measures and clean the cavity thoroughly. Inspect the bore for scoring, raised material, or damage before proceeding with installation.

Rationale. The primary risk in a drive-out method is bore damage caused by a cocked canister. Successful execution depends on continuous, reactive alignment control informed by tactile feedback rather than on incremental or scripted actions. The observed non-heroic retention fit (Section 6) makes this approach feasible, but only when handled with appropriate sensitivity and restraint.

Status and documentation. Figures 4a–4c document the executed extraction, including localized deformation at the drive-hole site, simultaneous application of counter-torque during tapping, and final removal. The removed canister was rendered unsuitable for reuse, but inspection confirmed that extraction forces were localized and that the crankcase bore was not subjected to damaging side loads.

11 Installation Execution and Observed Behavior

Installation of the replacement oil filter canister was performed in a single, deliberate operation following removal of the deformed original sleeve and inspection of the crankcase bore. The objective was to restore a clean geometric baseline while enforcing a controlled axial load path and avoiding secondary damage to the crankcase.

Prior to insertion, the distal end of the replacement canister was cleaned with gray Scotch-Brite to remove light surface oxidation and condition the surface for uniform contact during seating. The contact region was then lightly lubricated with engine oil to reduce insertion friction and mitigate the risk of galling.

As received, the replacement canister also carried an adhesive-backed BMW identification label on the outer surface. While appropriate for parts handling and inventory control, the label and its adhesive residue are incompatible with controlled press-fit installation. Complete removal proved nontrivial, requiring multiple applications of a citrus-based solvent (Goo-Gone) and careful scraping with a plastic blade to avoid surface damage. Final cleaning ensured a uniform metal-to-metal contact condition prior to insertion.

To further reduce required driving force, moderate external heat was applied to the surrounding crankcase using a heat gun (Fig. 4e). Heating was limited to raising the case to warm-to-touch temperature. The intent was to take advantage of differential thermal expansion between the aluminum crankcase and the steel canister, not to soften materials or alter interference characteristics. Lower ambient temperature further increased the available thermal expansion differential.

Axial insertion force was applied using a temporary driver assembled from existing BMW Airhead engine service tools (Fig. 4f). Although not a dedicated single-purpose driver, the stacked-tool arrangement was selected specifically to enforce a purely axial load path and to bear against the reinforced mouth region of the canister rather than the thin wall. This configuration provided adequate concentric guidance and allowed controlled tapping without introducing bending moments or off-axis loading.

The canister advanced smoothly with modest applied force, consistent with the light-retention behavior inferred from earlier observations. No abrupt resistance, stick–slip motion, or asymmetric engagement were encountered during insertion. In particular, there was no tendency for the canister to cock or bind as it approached its final position, supporting the conclusion that the later-style flared mouth geometry improves axial alignment and radial self-centering robustness during installation.

Insertion was halted at the previously marked reference line corresponding to the installed depth of the original canister (Fig. 4g). Final position was at, or marginally beyond, this reference, reflecting a conservative approach to depth control pending final measurement. Visual inspection into the installed canister (Fig. 4h) confirmed improved concentricity and uniform seating relative to the removed component.

At no point during the installation was corrective re-centering required, and no evidence of asymmetric resistance or elastic spring-back was observed after seating. These observations are consistent with a clean, undistorted bore and with the mechanically more forgiving mouth geometry of the later-style canister.

For completeness and future serviceability, a conceptual dedicated installation driver is described elsewhere in this work. While such a tool was not fabricated for this installation, the stacked factory-tool arrangement employed here satisfied the same functional requirements: axial load application, concentric engagement, and avoidance of thin-wall contact.

12 Execution Summary and As-Built Measurements

At the conclusion of this work:

- Two replacement oil filter canisters were received and verified to be visually consistent with BMW part `11 11 1 338 203`.
- The original canister was successfully removed using a field-expedient drive-out method, and the crankcase bore was subsequently inspected and cleaned.
- Although a dedicated canister installation driver could be designed in accordance with Table 1, the present installation was performed using a combination of BMW engine tools that satisfied the same functional requirements.
- Final depth control was achieved through direct measurement by transferring the wear mark from the original canister onto the replacement canister (Fig. 4d), and tapping the replacement canister into the bore until this reference mark was reached (Fig. 4g). This approach leverages the confirmed axial equivalence of the original and replacement canisters, with any residual variation accommodated using external shims.

Table 1: Suggested installation driver dimensions (later-style canister).

Feature	Suggested value	Notes
Material	6061-T6 aluminum or mild steel	Aluminum preferred (gentler contact)
Overall length	100 ––130 mm	Long enough to tap comfortably
Body diameter	45 ––55 mm	Stable striking surface
Pilot (recess) diameter	47.5 mm	Clearance fit inside nominal 48 mm ID
Pilot depth	4 ––6 mm	Enough to self-center
Annular bearing face OD	52 mm (max)	Must clear case opening
Annular bearing face ID	47.5 mm	Matches pilot diameter
Edge breaks	0.5 mm chamfer	Prevent gouging
Strike face	Flat and square	Optional slight crown acceptable

12.1 Measured Dimensions and Implications

Post-removal and post-installation measurements provide additional context for both the failure mechanism and the corrective strategy:

- The axial wear band on the original canister was measured at 11.59 mm from the mouth.
- Two independent measurements of the crankcase bore depth yielded 11.87 mm and 11.91 mm, confirming that seating to the original wear line retained margin to the bore floor.
- The removed canister measured approximately 137.87 mm in overall length.
- The replacement canister measured approximately 137.63 mm in overall length.

The small apparent difference in measured canister length is attributed to normal manufacturing tolerance and measurement uncertainty rather than to a designed or functional length change. For purposes of installation and depth control, the canisters are treated as equivalent in effective axial length.

Following installation, the canister depth measured an average of 3.90 mm from the crankcase face using a micrometer depth gauge, compared to a pre-removal value of approximately 3.60 mm. The increase in installed depth is attributed to unavoidable bore working during the interference event, extraction, and subsequent re-centering process. Depth measurements were repeated at multiple circumferential locations to confirm consistency and repeatability.

For a confirmed depth near 3.8 mm–3.9 mm, both the groove-depth relationship derived by Brooks and Brandon (*Airhead Garage*) and the tabulated shim guidance presented by Largiader indicate that a two-shim stack is appropriate. This configuration achieves the desired O-ring compression while preserving external observability and adjustment capability at the canister mouth.

13 Lessons Learned

- **Fastener length control is as critical as torque.** A correctly torqued fastener can still introduce unintended axial or radial loads if its length is wrong or if the true load path is misidentified.
- **Load paths matter more than component proximity.** Failures often originate not from the visibly damaged component, but from an adjacent structure that introduces force through an unexpected path.
- **Assumed press-fit behavior may differ substantially from reality.** Components described as "press-fit" may, in practice, be retained by modest interference and geometric constraint rather than by high-contact-stress engagement.
- **Rare service operations are especially vulnerable to documentation errors.** Fragmented institutional knowledge and persistent parts-fiche mislabeling materially increase the likelihood of assembly error, particularly for infrequently serviced components.
- **Visual and tactile cues require a correct mental model.** Resistance felt during assembly or service may indicate unintended mechanical interference rather than normal engagement or preload.
- **External oil leaks may serve as a protective failure mode.** Visible leakage can provide early indication of system distress and prevent more damaging internal bypass or starvation scenarios.
- **Tooling assumptions should be questioned rather than inherited.** The absence of obvious extraction features or purpose-built tools suggests that some "standard" service solutions may not exist in practice and should not be assumed.

- **Controlled leverage is not synonymous with brute force.** Moderate forces applied through long lever arms can generate significant moments; success depends on continuous alignment control and tactile awareness rather than force magnitude alone.

14 Conclusion

What initially appeared to be a conventional oil filter sealing failure was ultimately traced to a consequential violation of load-path intent. A single fastener of incorrect length introduced an unintended axial jacking load into a tolerance-sensitive system, displacing the oil filter canister and undermining O-ring preload despite otherwise correct assembly practices. The failure was not one of materials, design, or elastomer quality, but of geometry, force transmission, and assumption.

This investigation demonstrates the value of disciplined mechanical reasoning over pattern recognition. Symptoms that closely resemble well-known failure modes can arise from entirely different mechanisms when forces are routed through unexpected paths. Only by explicitly tracing geometry, tolerances, and reaction forces—rather than relying on visual cues or inherited service narratives—was the true cause revealed.

Several broader conclusions emerge. Components commonly described as "press-fit" may, in practice, rely on modest interference and geometric constraint rather than rigid fixation. Depth control in such systems is therefore a measurement problem, not a nominal-dimension problem. Likewise, scalar checks such as percent O-ring compression are useful only when their underlying assumptions—correct alignment, intact load paths, and stable geometry—are satisfied.

Finally, this case underscores the importance of honest documentation. Rare service operations, fragmented institutional knowledge, and even authoritative parts fiche errors create fertile ground for high-impact mistakes. Recording not only what failed, but *why* it failed, helps replace folklore with understanding and allows future work to be guided by mechanics rather than myth.

The system ultimately behaved exactly as physics dictates. The lesson is not that the BMW Airhead oil filter design is fragile, but that even robust designs can be compromised when invisible coupling between otherwise correct parts is introduced. Recognizing and respecting those couplings is the difference between routine service and unintended experimentation.

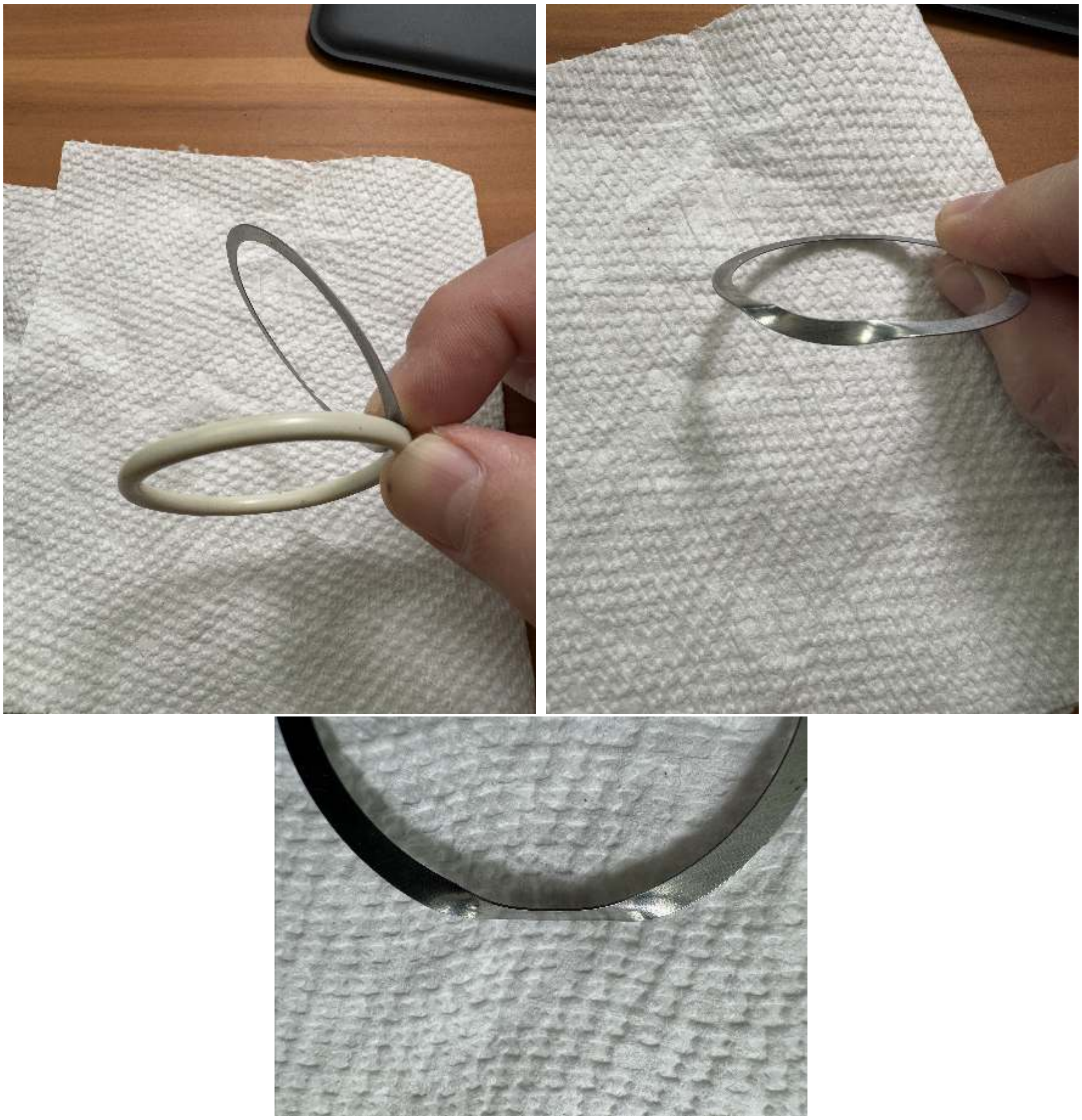

Figure 1: *O-ring and shim condition as found. The shim shows smooth, continuous plastic curvature in the region rendered unsupported by radial displacement of the canister mouth. The O-ring appears nominal in the images and is included for reference; its contribution to the observed deformation arises from load redistribution under geometric constraint rather than from visible material distortion.*

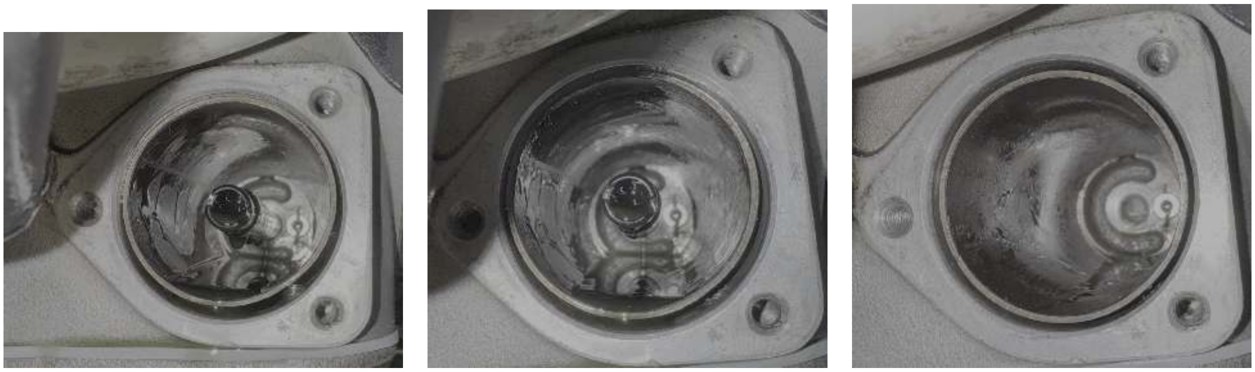

(a) *Localized deformation* *(b)* *Fastener removed* *(c)* *Mechanically re-centered canister*

Figure 2: *Canister displacement and recovery sequence, demonstrating dominant rigid-body motion about the distal press-fit region. (a) Localized deformation at the canister mouth caused by unintended radial jacking. Note the bolt protrusion visible in the lower-right quadrant (near the 5 o'clock position). (b) After fastener removal, partial elastic spring-back occurs, but full self-centering does not occur without an applied corrective moment. (c) Deliberate mechanical re-centering at the mouth restores nominal alignment. The central PIPE was removed at this stage to provide clearance for controlled levering without interference.*

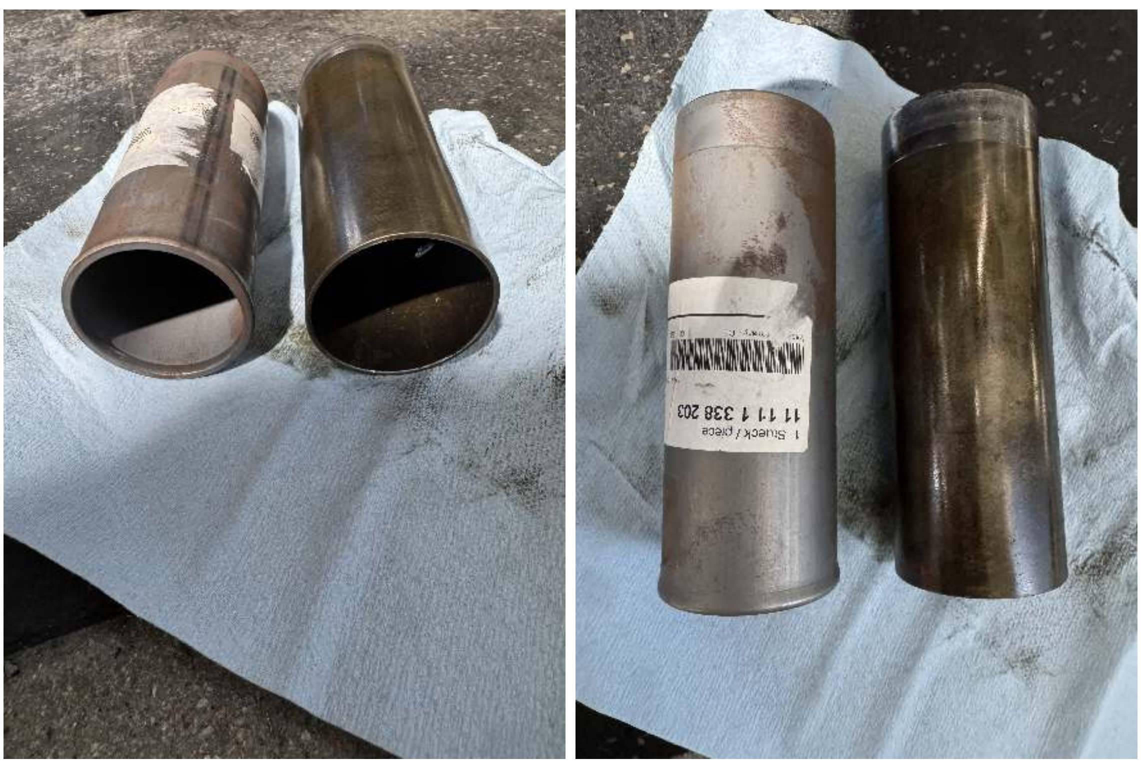

Figure 3: *Replacement canister mouth geometry and comparison. The formed mouth exhibits an initial outward flare, followed by inward rolling and final axial flattening, producing a broad, stiff sealing land for the O-ring and optional shims. Side-by-side comparison illustrates the mouth geometry and BMW part number presentation on the replacement canister.*

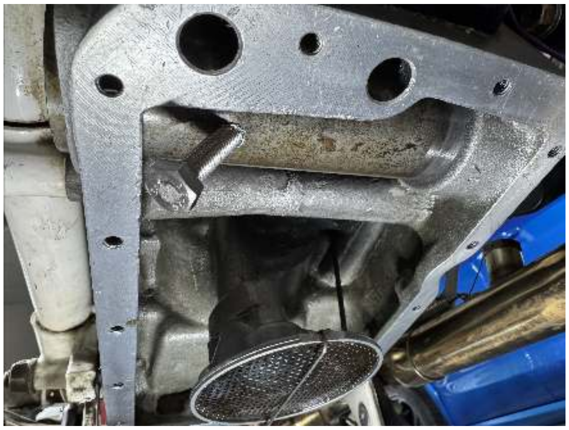

(a) *Localized wall deformation during drive-out tapping. The bolt orientation was perpendicular to the canister prior to tapping. Plastic deformation and bolt rotation within the thin sheet are unavoidable.*

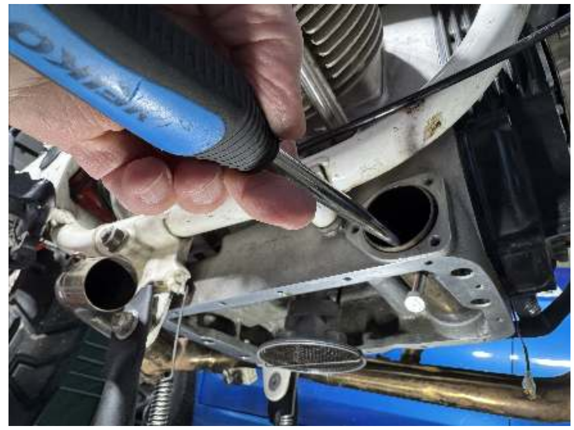

(b) *Counter-torque applied to maintain axial alignment and prevent bore damage.*

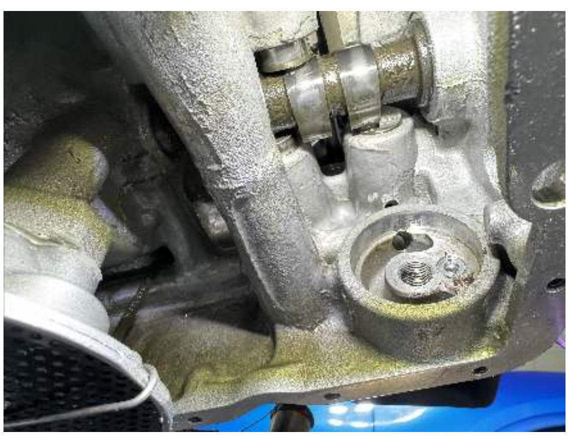

(c) *Canister removed after controlled tapping sequence.*

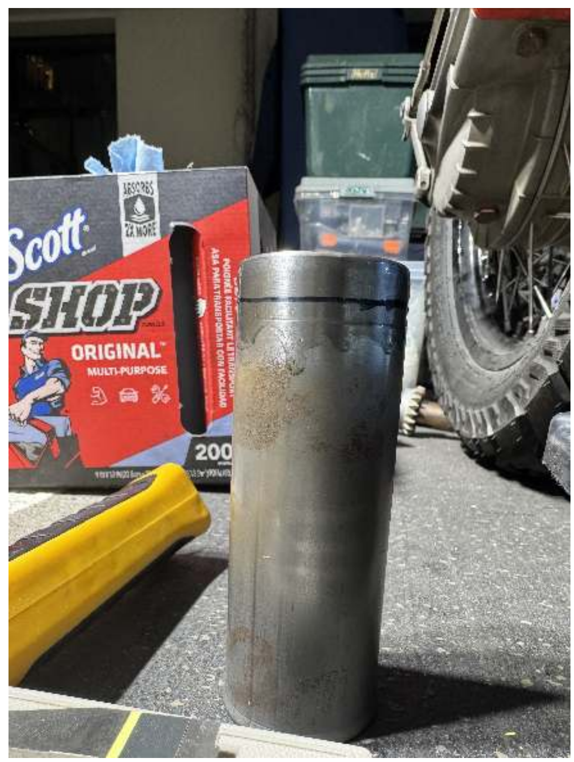

(d) *Replacement canister distal end cleaned and lightly oiled prior to insertion. Note the traced insertion depth check line.*

Figure 4: *Extraction and installation sequence (1 of 2).*

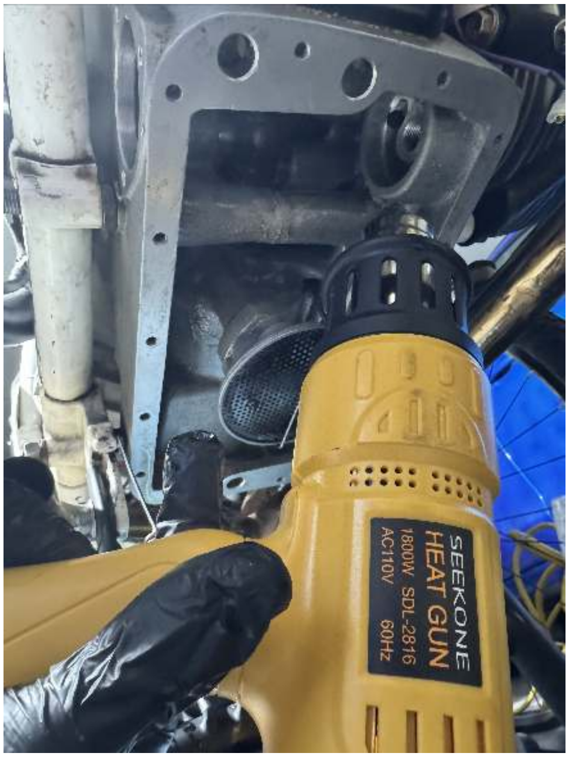

(e) *Crankcase warmed with heat gun to reduce insertion force via differential expansion.*

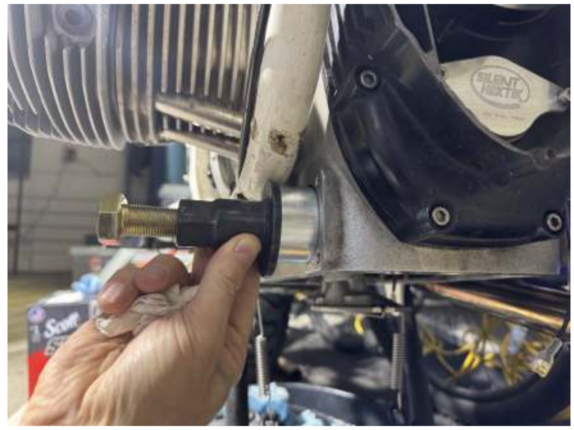

(f) *Temporary axial driver assembled from available engine tools.*

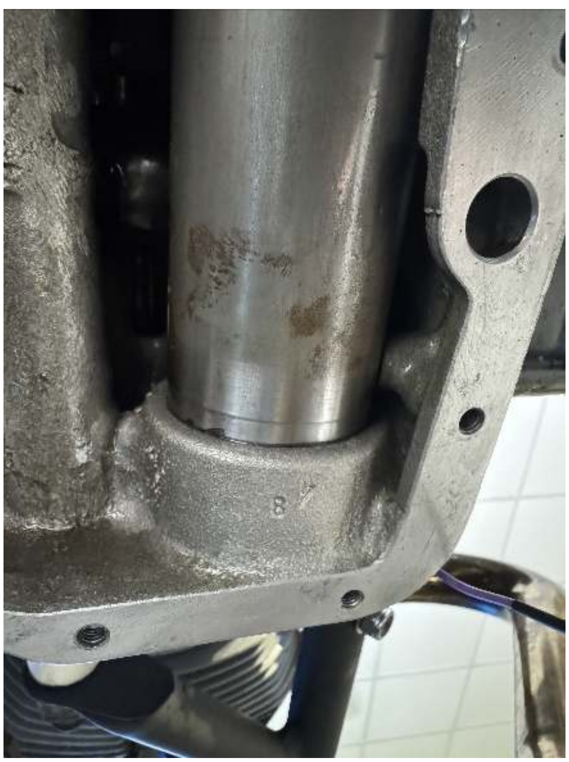

(g) *Final installed position relative to the reference depth mark.*

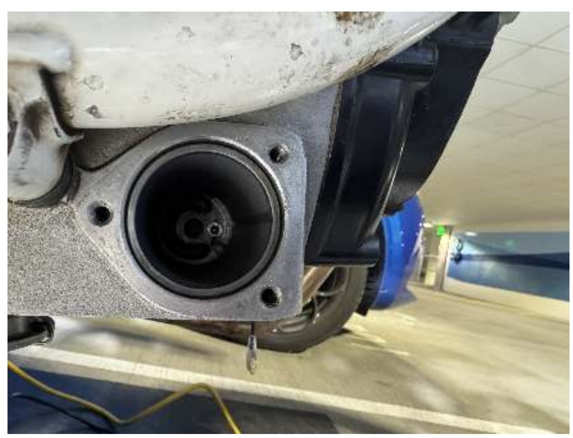

(h) *View into installed canister showing improved concentricity and self-centering.*

Figure 4: *Extraction and installation sequence (2 of 2).*